

# EFFECTS OF SAMPLING AND COMPRESSION ON HUMAN IRIS VERIFICATION

*S. Rakshit and D. M. Monro*

Department of Electronic and Electrical Engineering,  
University of Bath, Bath, BA2 7AY, United Kingdom  
{S.Rakshit, D. M. Monro} @bath.ac.uk

## ABSTRACT

The resilience of identity verification systems to subsampling and compression of human iris images is investigated for three high performance iris matching algorithms. For evaluation, 2156 images from 308 eyes are mapped into a rectangular format with 512 pixels circumferentially and 80 radially. For identity verification, the 48 rows nearest the pupil were taken and the images were subsampled by Fourier domain processing. Negligible degradation in verification is observed if at least 171 circumferential and 16 radial Fourier coefficients are preserved, corresponding to sampling at 342 by 32 pixels. With compression by JPEG 2000, improved performance is observed down to 0.3 bpp, attributed to noise reduction without significant loss of texture. To ensure that no algorithm is degraded, it is recommended that normalized iris images should be exchanged at 512 x 80 pixel resolution, compressed by JPEG 2000 to 0.5 bpp. This achieves a smaller file size than the proposed M1 biometric data interchange format.

## 1. INTRODUCTION

In this work we study the sampling requirements for reliable identity verification using human iris images, and evaluate the effect of data compression on the performance of several state of the art verification algorithms. Biometric authentication systems based on fingerprint, face, iris, etc. promise to provide a secure and reliable alternative to traditional techniques such as keys and codes [1,2]. Interest in the field of coding of iris images for recognition originated with Daugman's system using Gabor wavelets [3, 4]. Since then there has been much activity by research groups such as Wildes [5], Boles [6], Tan et. al. [7] and Monro [8].

Evaluation of biometric systems often requires large volumes of data to be collected, stored and shared [9]. The use of a standard compression algorithm such as JPEG 2000 would provide for an open system whereby the data may be readily reconstructed by all users. In lossy compression systems quality is lost as the compression ratio increases [10] and the effect of compression on iris recognition has not been previously reported.

The paper is organized as follows. An overview of the iris recognition algorithms considered is given in Section 2. Section 3 studies the sampling requirements for reliable identity verification from the point of view of frequency domain processing. The effects of JPEG 2000 compression on normalized iris images and verification performance are illustrated in Section 4. Finally conclusions are drawn and standards recommendations for sampling and interchange of iris images are made in Section 5.

## 2. IDENTITY VERIFICATION

### 2.1 Overview of Iris Recognition Algorithms

A brief summary of recognition algorithms developed by Daugman, Tan and Monro follows. In Daugman's method, the iris image is filtered using a family of multiscale Gabor filters [3, 4]. The phase structure is then demodulated into a sequence of complex-valued phasors which are projected onto a four-quadrant complex plane to generate a binary iris code. Tan, on the other hand, generates a bank of 1D intensity signals from the iris images [7]. These are then filtered with the help of a special class of wavelets and the position of local sharp variations is recorded to form the feature vector. The Monro Iris Transform (MIT) divides the image into patches and utilizes one-dimensional frequency variations between them to generate the feature vectors [8].

### 2.2 Pre-processing and Normalization

Common to all the above algorithms is the initial pre-processing stage of eye-image normalization. In the present work this is achieved by first finding the approximate position of the pupil by detecting transitions in the vertical and horizontal grey level profiles of the image. A binary image obtained using the Canny edge detector is subjected to morphological operations to locate the inner and outer boundaries of the iris. This is then mapped from polar coordinates to a 512 x 80 pixel rectangular image to provide a normalized spatial template which compensates for the effects of iris dilation and contraction. The non-uniform background illumination is finally homogenized and the 512 x 48 pixel image nearest the pupil is selected for coding, as in Figure 1.

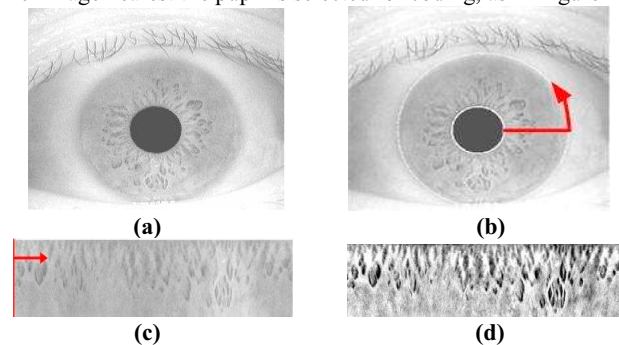


**Figure 1.** a) Typical human eye image; b) iris outlines detected; c) resampled: polar – cartesian; d) intensity enhanced.

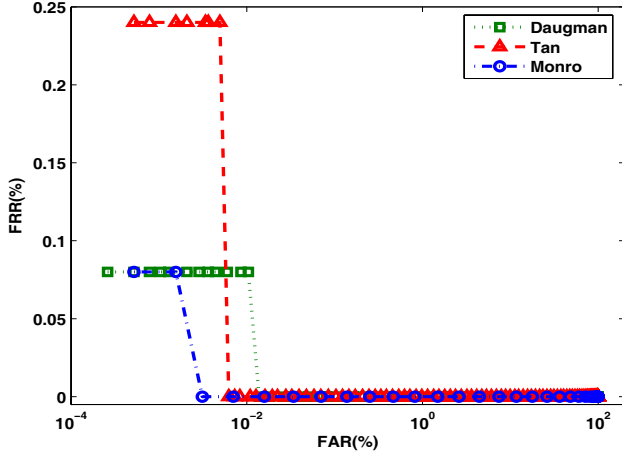


**Figure 2.** ROC Curves for three algorithms with original normalized images.

### 2.3 System Performance

System performance is usually described by a Receiver Operating Characteristic (ROC) [1] in which the False Rejection Rate (FRR) is plotted against the False Acceptance Rate (FAR) to indicate the trade-offs that can be achieved between the two error rates. It is obtained in Figure 2 for the three algorithms considered by varying the matching threshold in each.

The images used were a set of 2156 images of 308 eyes from the CASIA Database [11]. The number of images of each eye is not consistent. In evaluating the FAR, there were 378224 ( $1232 \times 307$ ) trials while the FRR estimates are made from 1232 trials.

In Figure 2 the ROC graph is carried as close to the Y-Axis as the amount of data will permit. A single False Rejection in this data gives a FRR of  $8 \times 10^{-4}$  %, which for the Monro Transform first occurs at a FAR of  $2 \times 10^{-3}$  % and is as many as can be triggered. Modeling it by a binomial distribution it can be said with 90% confidence that the failure rate lies between  $1.04 \times 10^{-3}$  % and  $3.76 \times 10^{-3}$  %. To narrow this range of uncertainty, evaluation on much larger data sets is required. Our implementation of the Daugman and Tan algorithms follows their latest published papers and without any undocumented optimizations.

### 3. FREQUENCY CONTENT AND SUBSAMPLING

As is plainly evident, iris images have higher frequency content circumferentially than they have radially. As a preliminary indication of the relative requirements of circumferential and radial sampling, spectral analysis by a one-dimensional FFT in each direction was carried out. In the circumferential direction, the data is naturally periodic, so no windowing was required. Figure 3a. shows the average over 48 rows of the normalized power spectrum for the 2156 images. For radial sampling, a 1/8th tapered cosine window was used at each end of each column of pixels prior to radial spectral analysis. The normalized ac power spectrum averaged over all 512 columns of the 2156 images is shown in Figure 3b. It is clear that the requirements for circumferential sampling are higher than for radial sampling. For example, 99% of the averaged image power is contained within 143 coefficients circumferentially but only 8 radially. It will be shown below that

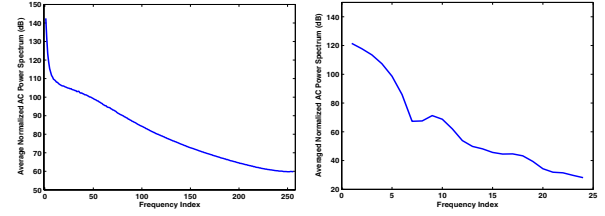


**Figure 3.** Average normalized ac power in the a) Circumferential, and b) Radial Direction of normalized iris images.

more than 99% is required in order that the verification performance of the three systems studied is not degraded.

To evaluate the effects of sampling directly on verification, the normalized iris images were subsampled to various degrees to emulate low resolution image capture. Both spatial and frequency domain approaches were used. In the spatial case, multiple pixels were replaced by their mean graylevel. This method, applied in both directions, simulates low resolution CCDs but is restricted to integer subsamplings. The normalized image, of size  $512 \times 48$ , was subsampled to 256, 128 and 64 columns, and 24, 16 and 8 rows. All combinations were explored and as expected performance degradation occurred in all cases. The degradations are more pronounced in the horizontal (circumferential) direction for similar down-sampling ratios. As downsampling by a factor of 2 was too severe, it was necessary to examine non-integer downsampling ratios between 1 and 2.

To achieve this the inverse Fourier transform of a reduced frequency domain was used out to obtain reduced images. The effect of aliasing was simulated by overlapping symmetrical high-frequency regions and adding them prior to clipping. To eliminate frequencies above a certain value, say  $X$ , overlapping must be done equally on either side of  $X$  up to the mid-frequency. This method can be extended to two dimensions by considering conjugate symmetry and applying superimposition in both directions as illustrated in Figure 4. Same-factor subsampling was used to implement all algorithms accurately. Factors ranging from 1.20 to 4.00 were tried giving image heights ranging from 12 to 40 pixels in steps of 4. Figure 5 shows acceptable system performance below a factor of 1.50, where the image size is  $32 \times 342$ .

The power content of the images was analyzed as a percentage of the total power of the original image. 99% of the image power is retained to a subsampling factor of 3 as can be seen in Figure 6. In

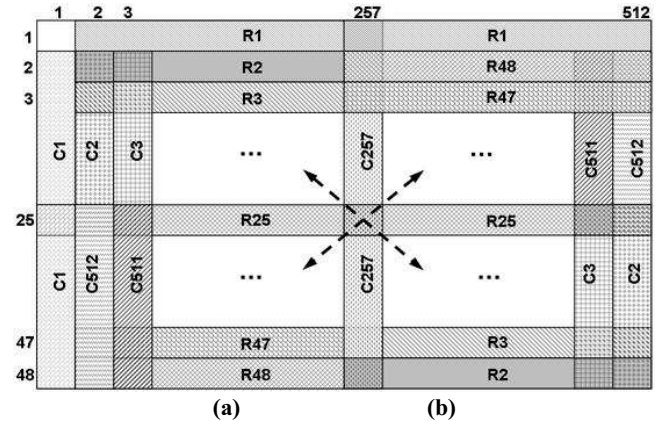


**Figure 4.** Symmetry of Coefficients in the 2D FFT

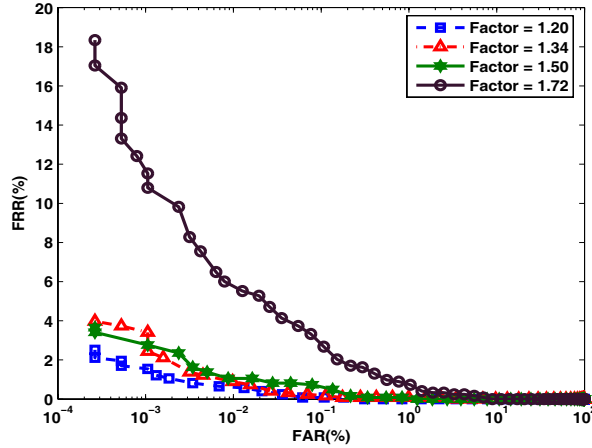


**Figure 5.** Effects of subsampling on the MIT ROC curve for various factors in the frequency domain

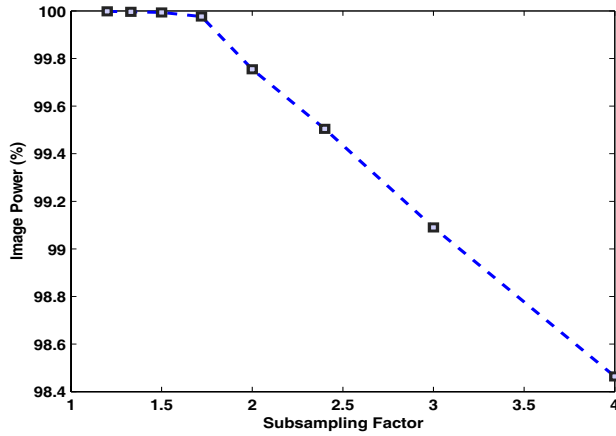


**Figure 6.** Effect of subsampling on the image power.

particular the image power at the acceptable subsampling factor of 1.50 is 99.994%. Going back to the initial spectra of Figure 3, we see that for robust recognition, a minimum of 16 radial coefficients and 171 circumferential ones are required in the frequency domain. For subsampling ratios higher than 1.50, the ROCs are degraded beyond any practical use. The use of low resolution sensors for image acquisition could therefore prove to be a major hindrance in achieving acceptable error rates, and the same applies to excessive down-sampling as a size-reduction measure. As will be shown later, JPEG2000 compression produces far better results with significantly lower memory requirements.

#### 4. COMPRESSION BY JPEG2000

To evaluate the effect of compression on iris images, the JPEG 2000 codec Kakadu Version 4.3 was used to compress and decompress all the normalized irises in the CASIA database. The use of wavelet technology in JPEG 2000 results in more efficiently compressed images with smaller errors than in previous standards for image compression [12]. The compression experiment was carried out over a range of bit-rates between 0.1 bpp, where significant degradation is expected, to 1 bpp, where images are widely accepted to be visually lossless. As the compression was



**Figure 7.** Normalized iris images compressed at 1.0 bpp, 0.5 bpp and 0.1 bpp.

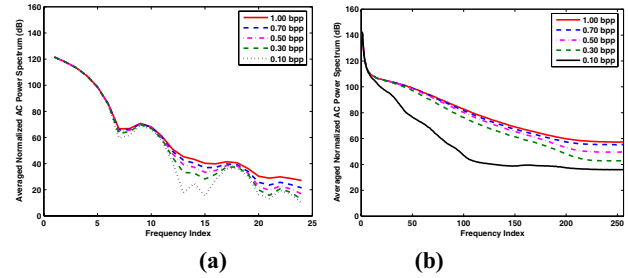


**Figure 8.** Average normalized ac power spectrum for various compression rates in the a) Circumferential, and, b) Radial direction of normalized images.

carried out from 1.0 bpp downwards, it was observed visually that the essential iris texture was retained to as low as 0.3 bpp despite some visible smoothing. Beyond that, the loss in texture detail is significant and at 0.1 bpp the image is blurred beyond recognition. Sample normalized images compressed at 1.0, 0.5 and 0.1 bpp are shown in Figure 7 to demonstrate this effect.

The spectral analysis, carried out for uncompressed images in section 3 above, was repeated for all compression values on the images after decompression. Figure 8 shows the loss in power of the FFT coefficients over the range of compression rates for circumferential and radial analysis. It is observed that 99% of the power is preserved down to 0.2 bpp compression both circumferentially and radially.

To assess the effect of image compression on the verification algorithms, images after compression and decompression were used to form both the registered and matching iris codes over the range of compression studied. Three decompressed images of each of the 308 eyes were coded into the registered database and the remaining 1232 decompressed images were coded and matched against them. The ROC curves generated for all compression rates for the three algorithms reveal interesting results. As the compression ratio increases, the system performance improves down to a bit rate of 0.5 bpp where the total retained image power is found to be 99.84%. This result may be a consequence of the fact that light to moderate compression is well-recognized as a strategy for image denoising. Moderate compression therefore produces better performance curves due to noise-removal without destroying the features of image texture that are important for verification. The ROC curves are acceptable up to 0.3 bpp, but beyond that the degradation becomes severe so that at 0.1 bpp the FAR and FRR rates are too high to be of any practical use. Curve combinations for 0.5 bpp are shown in Figure 9 to illustrate this effect.

The Correct Recognition Rate (CRR), which is the ratio of correctly identified subjects to the total population remains at 100% for all algorithms down to bit-rates as low as 0.3 bpp. In our studies we observe that a more meaningful indication of where the

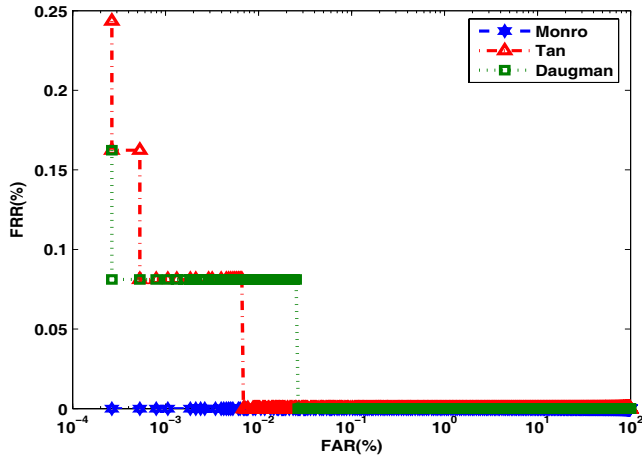


**Figure 9.** ROC Curves for the three algorithms for images compressed at 0.5 bpp

verification performance begins to degrade is the FAR when the first False Rejection occurs. This is a measure of the extent to which the matching threshold may be reduced without the occurrence of any false rejections. A lower value of this threshold is desirable as it keeps the false acceptance rate to a minimum. Figure 10 clearly demonstrates that significant degradation caused by compression occurs only from 0.2 bpp downwards.

## 5. CONCLUSIONS

The technology of iris coding is at an early stage, due in no small part to commercial constraints arising from generic patents. It is important that any standardized iris exchange format should err on the side of caution in specifying a compaction ratio. Because iris normalization plays a key role in the performance of any verification system, for fair comparisons to be made verification algorithms should be compared on images which are already normalized. The current proposal for the M1 human iris in polar format subsamples a normalized iris to 256 circumferential and 8 radial pixels [13]. The spectral analysis carried out here suggests that this should preserve 99% of the image power radially and more circumferentially. However the subsampling studies suggest

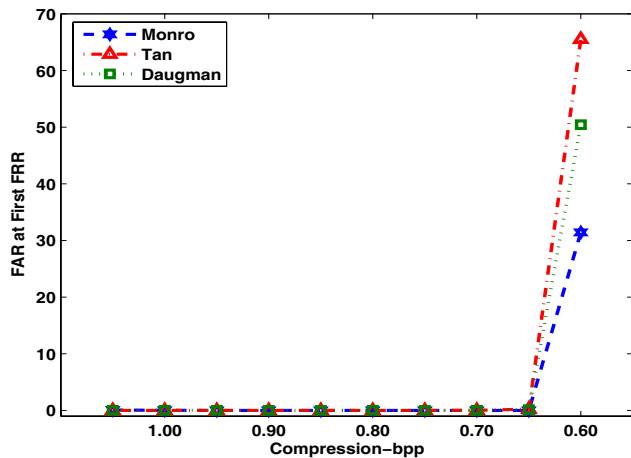


**Figure 10.** FAR at First Rejection as a function of compression for the three algorithms considered.

that 99% of radial power is not sufficient. Further analysis shows that a minimum of 171 Fourier coefficients are required circumferentially and 16 radially to preserve 99.99% of the image power and give acceptable ROC curves which are not degraded for the verification algorithms studied. For practical and efficient image processing purposes, it is recommended that the normalized iris image size be fixed at 80 rows and 512 columns.

Moderate compression of normalized iris images, by JPEG2000 to around 0.5bpp, lead to improved ROC curves due to noise removal without detrimental effects on image texture. In the light of this finding, it is recommended that JPEG2000 compression at 0.5 bpp be used for the interchange of iris images to allow for future development of more accurate codes. If required, compression rates as low as 0.3 bpp could be used without degrading the performance significantly.

## 6. REFERENCES

- [1] A. K. Jain, A. Ross, and S. Prabhakar, "An Introduction to Biometric Recognition," IEEE Trans. Circuits and Systems for Video Tech., vol. 14, pp. 4 - 20, 2004.
- [2] A. Jain, R. Bolle, and S. Pankanti, "Biometrics: Personal Identification in Networked Society," Kluwer Academic Publishers, 1999.
- [3] J. Daugman, "High confidence visual recognition of persons by a test of statistical independence," IEEE Trans. on Pattern Analysis and Machine Intelligence, vol. 15, pp. 1148 - 1161, 1993.
- [4] J. Daugman, "Statistical richness of visual phase information: Update on Recognizing Persons by Iris Patterns," Inter. Journal of Computer Vision, vol. 45, pp. 25-38, 2001.
- [5] R. P. Wildes, "Iris recognition: an emerging biometric technology," Proc. of the IEEE, vol. 85, pp. 1348 - 1363, 1997.
- [6] W. W. Boles and B. Boashash, "A Human Identification Technique Using Images of the Iris and Wavelet Transform," IEEE Transactions on Signal Processing, vol. 46, pp. 1185 - 1188, 1998.
- [7] L. Ma, T. Tan, Y. Wang, and D. Zhang, "Efficient iris recognition by characterizing key local variations," IEEE Trans. on Image Processing, vol. 13, pp. 739 - 750, 2004.
- [8] D. M. Monro and D. Zhang, "An effective human iris code with low complexity," presented at Proceedings of IEEE International Conference on Image Processing, 2005.
- [9] J. L. Wayman, "Fundamentals of Biometric Authentication Technologies," Int. Journal of Image and Graphics, vol. 1, pp. 93-113, 2001.
- [10] D. Taubman and M. Marcellin, "JPEG2000: Image Compression Fundamentals, Standards and Practice," The Kluwer International Series in Engineering and Computer Science, 2002.
- [11] CASIA Iris Image Database, <http://www.sinobiometrics.com>
- [12] D. Santa-Cruz and T. Ebrahimi, "An analytical study of JPEG 2000 functionalities," IEEE Proceedings of International Conference on Image Processing 2000, vol. 2, pp. 49-52, 2000.
- [13] F. Podio and C. Soutar, "Iris Image Interchange Format," INCITS - American National Standard for Information Technology 2003.